Prediction of SSVEP-based BCI performance by the resting-state EEG network

2013 J. Neural Eng. 10 066017

(http://iopscience.iop.org/1741-2552/10/6/066017)

J. Neural Eng. **10** (2013) 066017 (10pp) doi:10.1088/1741-2560/10/6/066017

Prediction of SSVEP-based BCI performance by the resting-state EEG network

Yangsong Zhang, Peng Xu, Daqing Guo and Dezhong Yao[1]

Key Laboratory for NeuroInformation of Ministry of Education, School of Life Science and Technology, University of Electronic Science and Technology of China, Chengdu, 610054, People's Republic of China

E-mail: dyao@uestc.edu.cn

Received 19 August 2013
Accepted for publication 14 October 2013
Published 27 November 2013
Online at stacks.iop.org/JNE/10/066017

Abstract

Objective. The prediction of brain–computer interface (BCI) performance is a significant topic in the BCI field. Some researches have demonstrated that resting-state data are promising candidates to achieve the goal. However, so far the relationships between the resting-state networks and the steady-state visual evoked potential (SSVEP)-based BCI have not been investigated. In this paper, we investigate the possible relationships between the SSVEP responses, the classification accuracy of five stimulus frequencies and the closed-eye resting-state network topology. *Approach.* The resting-state functional connectivity networks of the corresponding five stimulus frequencies were created by coherence, and then three network topology measures—the mean functional connectivity, the clustering coefficient and the characteristic path length of each network—were calculated. In addition, canonical correlation analysis was used to perform frequency recognition with the SSVEP data. *Main results.* Interestingly, we found that SSVEPs of each frequency were negatively correlated with the mean functional connectivity and clustering coefficient, but positively correlated with characteristic path length. Each of the averaged network topology measures across the frequencies showed the same relationship with the SSVEPs averaged across frequencies between the subjects. Furthermore, our results also demonstrated that the classification accuracy can be predicted by three averaged network measures and their combination can further improve the prediction performance. *Significance.* These findings indicate that the SSVEP responses and performance are predictable using the information at the resting-state, which may be instructive in both SSVEP-aided cognition studies and SSVEP-based BCI applications.

(Some figures may appear in colour only in the online journal)

1. Introduction

The steady-state visual evoked potential (SSVEP) is a periodic response evoked by a repetitive visual stimulus with a frequency above 4 Hz. It has the same fundamental frequency as the stimulus as well as its harmonics [1]. SSVEP has been widely used to study the neural processes underlying rhythmic brain activities in cognitive and clinical neuroscience [2]. Because of the high signal–signal ratio and robustness, the SSVEP-based brain–computer interface (BCI) has become an important system in the BCI community [3–5]. However, up to now the underlying mechanisms which account for the differences in SSVEP responses across subjects still need to be explored; few works in the literature probe into these aspects.

The brain is a complex network consisting of a large number of functionally and structurally interconnected regions. There is accumulating evidence that indicates the value of brain network topology for understanding cognitive

[1] Author to whom any correspondence should be addressed.

processes and diseases [6–9]. Brain network topology can be derived by theoretical graph analysis. Usually, a brain network can be constructed by calculating the functional connectivity between the concerned brain regions. Functional connectivity is defined as the statistical dependence of neuronal activity patterns between anatomically separated brain regions [10]. Various measures, such as correlation, synchronization likelihood, coherence and phase lag index can be used to calculate the functional connectivity [8, 11–13]. The construction of brain networks during rest is a hot topic in the neuroscience community. Studies have shown during rest the brain is not idle, but rather that it shows an amount of spontaneous activity that reflects the brain's potential processing abilities [8, 14]. Recently, intensive statistical analysis has revealed that the topology of a resting-state brain network has significant associations with cognitive functions and performance. [9, 11, 12].

On the other hand, many resting-state measures have been demonstrated to be relevant to BCI performance [15–17]. For example, Blankertz *et al* showed the averaged power spectral densities (PSD) of two channels from the 2 min of open-eyed resting-state EEG data can be predictors of motor imagery BCI performance [17]. Fernandez-Vargas *et al* also showed that inter-individual baseline resting-state EEG measures (PSD in specific frequency bands) were correlated with assisted closed-loop SSVEP-based BCI performance [16]. However, so far little is known about the role of resting-state brain networks in BCI. In this study, we try to investigate the significance of resting-state brain network topology of the stimulus frequencies in the SSVEP responses and the SSVEP-based BCI classification performance. To this end, five different frequencies are adopted to explore our goals. Interestingly, we found that the resting-state network topology is related to both the SSVEP responses and the performance of SSVEP-based BCI.

2. Materials and methods

2.1. Participants

Twelve healthy right-handed adults (two females, age range: 20–27 yr, mean (SD) age was 22.5(2.2) yr) with normal or corrected to normal vision participated in this study. All participants signed an informed consent form before participating in the study. These subjects had no historical record of any epileptic seizure. The study was approved by the Human Research and Ethics Committee, University of Electronic Science and Technology of China.

2.2. EEG data acquisition

All data were collected from 64 Ag–AgCl electrodes extended to a 10–20 system (Brain Products GmbH, Germany). The data were sampled at 1000 Hz with an online bandpass filter between 0.01–100 Hz and a 50 Hz notch filter for the line frequency interference (50 Hz in China). The impedance for all electrodes was kept below 10 kΩ. Frontal vertex (i.e. FCz) was the reference electrode, and AFz served as the ground electrode during recording. To control for eye movement artifacts, horizontal and vertical electro-oculograms (EOGs) were recorded from electrodes placed above the left eye and at the outer canthus of the right eye, respectively.

2.3. Experimental procedure

For each subject, 2 min of closed-eye resting-state data were collected. After that, each of five frequencies, i.e. 7.5, 10, 12, 15 and 20 Hz were used to collect SSVEP data for 1 min. The stimulus sequence of the five frequencies was random across the subjects. The subjects had a 2–3 min break between each experiment to relax. The stimulus flickers were controlled by a computer through a control program written in C++ builder based on Windows DirectX API. The size of the stimulus was a 2×2 cm^2, with a duty cycle 0.5, 0.5, 0.6, 0.5 and 0.5 for the five frequencies, respectively. A laptop with a 13″ screen and a refresh rate of 60 Hz was used to present stimuli. During the experiment, the subjects were seated in a comfortable armchair, about 60 cm away from the center of the monitor. Subjects were requested to gaze binocularly at each flickering stimulus. The experiment lasted for about 1 h.

2.4. Data processing

2.4.1. Data preprocessing. To eliminate the signal excursion, the EEG data were filtered with 1–100 Hz, and then resampled to 250 Hz. To reject electrodes with a preponderance of noise resulting from insufficient contact with the scalp, two electrodes, TP9 and TP10 were eliminated from the study due to excessive artifact.

For each subject, we chose the first seven non-overlapping artifact-free (common artifacts such as eye blinks, eye movements and muscle activities, amplitude exceeded 100 μV) epochs of 10 s from the resting-state data, and the first three to five non-overlapping and artifact-free epochs of 4 s from the SSVEP data. After these pre-processing procedures, all data were re-referenced to zero reference by the reference electrode standardization technique (REST) (Free software download at www.neuro.uestc.edu.cn/rest/index.asp) [18].

2.4.2. SSVEP data processing. In this work, the SSVEP data processing is divided into two steps. First, we measured the SSVEP response under each frequency for each subject. Second, because stimulus frequencies are always not across a wide frequency band (7.5 Hz–20 Hz), we calculated the classification accuracy by pooling the data of the four frequencies (7.5, 10, 12 and 15 Hz) together for each subject. To lower the possible effect of background across subjects, we expressed SSVEP responses as the signal-to-noise ratio (SNR) based on the fast Fourier transform (FFT) [19]. The SNR was defined as the ratio of the power of the stimulus frequency divided by the mean power value of the 1 Hz band which centered on the stimulus frequency but excluded the stimulus frequency itself. For each subject, the SNRs for the nine electrodes (P3, Pz, P4, PO3, POz, PO4, O1, Oz, O2) located in the occipital area were calculated in each epoch, then SNRs were further averaged across the epochs and electrodes for each stimulus frequency.

To implement classification, we used the canonical correlation analysis (CCA) which is one of the methods that can provide satisfactory results for SSVEP-based BCI [20–22]. This method uses the multivariable statistical method CCA to calculate the correlation coefficients between the multiple electrodes EEG and the reference signals. The data from the nine electrodes mentioned above were chosen as the input of CCA. A study has shown that there is no significant influence for the number of harmonics on the frequency recognition for CCA. In order to avoid the interference between the harmonic frequencies, we just chose the first harmonic when creating the reference data matrix. A 2 s time window was chosen for the classification as in other related works [20, 21, 23]. Accordingly, there were two classification operations for each of the 4 s long data epochs.

2.4.3. Resting-state network calculations. To reduce volume conduction influence, 19 standard electrode positions Fp1, Fp2, F7, F3, Fz, F4, F8, T7, C3, Cz, C4, T8, P7, P3, Pz, P4, P8, O1, O2 were chosen as the nodes to construct the networks. The coherence was adopted to measure the functional connectivity between a pair of electrodes. For each subject, we calculated five coherence matrices corresponding to the five frequencies in each epoch of the resting-state data respectively. Then the coherence matrices of each frequency were averaged across epochs.

The coherence was always nonzero resulting in a too dense network. Therefore, in order to reduce some spurious edges, we reduced the total edges based on the sparsity threshold. Sparsity is defined as the ratio of the total number of edges divided by the maximum possible number of edges in a network [6, 7]. The criterion to choose the threshold was that all brain networks across all subjects were fully connected while minimizing the number of false-positive edges with the sparsity value. In essence, this method was used to keep the edges with large connection weights and delete some edges where connection weights were small. With this strategy, the resulting networks had the same number of nodes and edges [6, 7]. In the current work, we determined the sparsity value based on all the averaged matrices of the five frequencies from the 12 subjects under all the frequencies.

For convenience, we denoted the new averaged matrices after the reduced artificial links based on the sparsity value as the resting network.

2.4.4. Resting network topology measures. To measure the resting network topology, we first calculated the mean functional connectivity of each resting network, and then used the theoretical graph analysis to evaluate the topological properties, i.e. the clustering coefficient and the characteristic path length for each resting network. The mean functional connectivity of each resting network was defined as the mean coherence between all the possible coherence connections between each pair of electrodes in each resting network. These two topological properties were calculated by using the Brain Connectivity Toolbox [24]. It should be noted that we focused on weighted network analysis in this study.

In a weighted network ($N \times N$), the clustering coefficient of a node i represents the likelihood that the direct neighbors of the node are also connected with each other [25], and it is calculated as follows:

$$C_i = \frac{\sum_{j,h\in N} (w_{ij} w_{ih} w_{jh})^{1/3}}{k_i(k_i - 1)}, \tag{1}$$

where w_{ij} is the weight between nodes i and j in the network, and k_i is the degree of the node i. Note that w_{ij} is the coherence between two electrodes in this paper. Then, the network clustering coefficient is defined as the average of the clustering coefficients of all nodes:

$$C = \frac{1}{N}\sum_{i\in N} C_i. \tag{2}$$

It is a measure of the extent of the local density or cliquishness of the network [26].

The characteristic path length which quantifies the level of global communication efficiency of a network is measured by a harmonic mean length between different pairs [27], to handle the possible disconnected edges. It is calculated as follows:

$$L = \frac{1}{1/(N(N-1)) \sum_{i=1}^{N} \sum_{j\neq i}^{N} 1/L_{ij}}. \tag{3}$$

Here L_{ij}, is the shortest path length between nodes i and j. The length of each edge is defined as the inverse of the edge weight, $1/w_{ij}$.

3. Results

3.1. Individual differences in SSVEP responses (SNR)

The SSVEP responses SNR of different subjects under the five stimulus frequencies are shown in figure 1. The differences of each frequency exist among subjects. These inter-individual variabilities provide chances for us to explore the relations between the SNRs and the underlying network measures.

3.2. The relationship between SNRs and mean functional connectivity

Based on the procedure mentioned above, the sparsity value in the present work was determined as 0.77. In the following studies, we used this threshold value to reduce the spurious connections of the averaged networks of each frequency for each subject to get the resting networks, and then further calculated the topological measures. After these procedures, we investigated the relationship between SNRs and network topology using Pearson's correlation analysis.

Firstly, we focused on the relationship between the SNRs and the mean functional connectivity of each frequency. The detailed correlation information was listed in table 1 and figure 2(a). Interestingly, under each frequency condition, the mean functional connectivity showed significantly negative correlation with the SNRs, despite a marginal significant correlation under 10 Hz, probably due to interference from the stronger alpha background activities. Furthermore, we found that the averaged functional connectivity across the five resting networks showed a significantly negative correlation with the

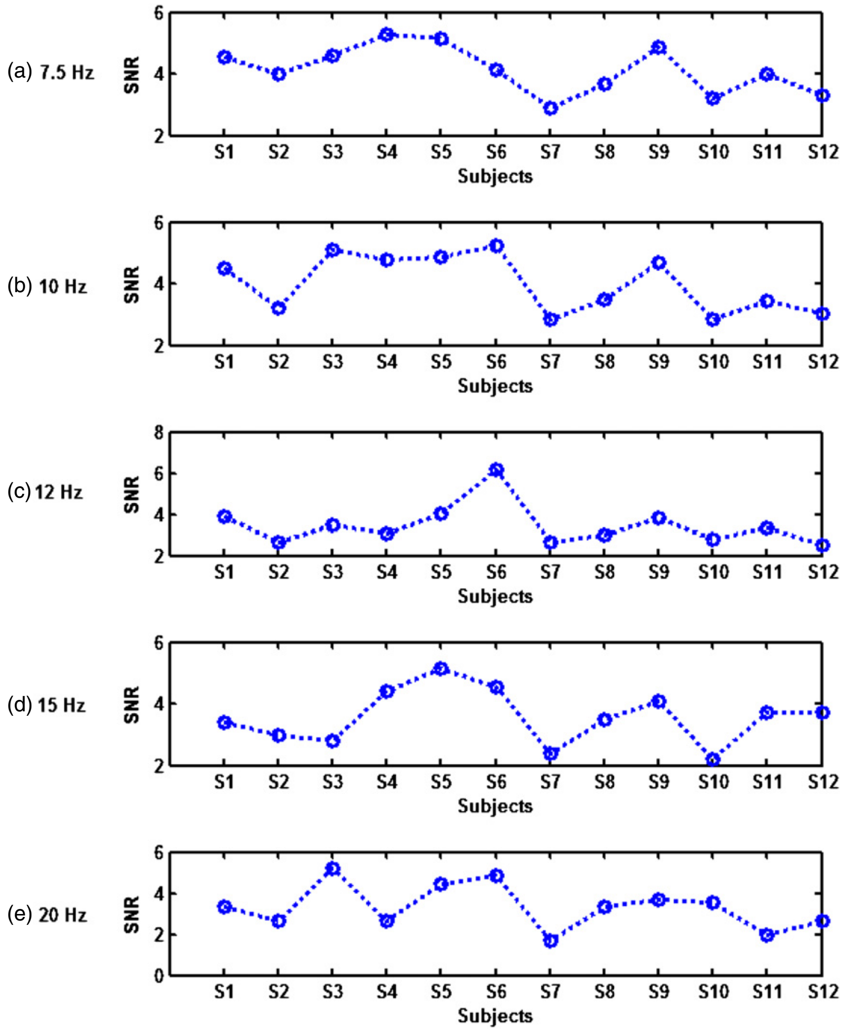

Figure 1. The SNRs of the five frequencies across different subjects.

Table 1. The correlation of the mean functional connectivity of each frequency and the SNRs. r denotes the correlation coefficient and p denotes the significant level of the correlation coefficient.

Frequency	r	p
7.5 Hz	−0.789	0.002
10 Hz	−0.569	0.054
12 Hz	−0.745	0.005
15 Hz	−0.731	0.007
20 Hz	−0.742	0.006

average SNRs of the five frequencies across the subjects, as shown in figure 2(d).

In order to specify the contribution of each connection to the SNRs under each frequency, we computed the correlation coefficients between the strengths of each connection and the SNRs across subjects. The topology maps are shown in figures 2 and 3. All the links in figure 2 denote the connections which are positively correlated with the SNRs. These links are sparse, and widely distributed without any specific patterns. The connections which are negatively correlated with the SNRs are denser than the positively correlated links. In order to clearly show the main contributors, we only plotted the links of which the absolute values of the correlation coefficients are equal to or larger than 0.4. In figure 3, it seems that the main contributors may be the connections from the occipital to frontal regions. In one of our recent studies, we also found that the long connections from the parietal-occipital to frontal region under the flickering stimulus were significantly correlated with the SNRs across subjects [28]. In addition, Srinivasan *et al* reported that the occipital and frontal cortices were the two main sources of SSVEP [29]. These findings may indicate that the occipital and frontal cortices contribute more to the high SNRs, and further contribute to the correlations between the network measures and the SNRs.

3.3. The relationship between SNRs and topological properties

Similarly to the relationship between the mean functional connectivity and the SNRs, we found interesting results between the SNRs and the two topological properties as shown in table 2 and figures 4(b), (c). The SNRs of the four frequencies (7.5, 12, 15 and 20 Hz) were significantly

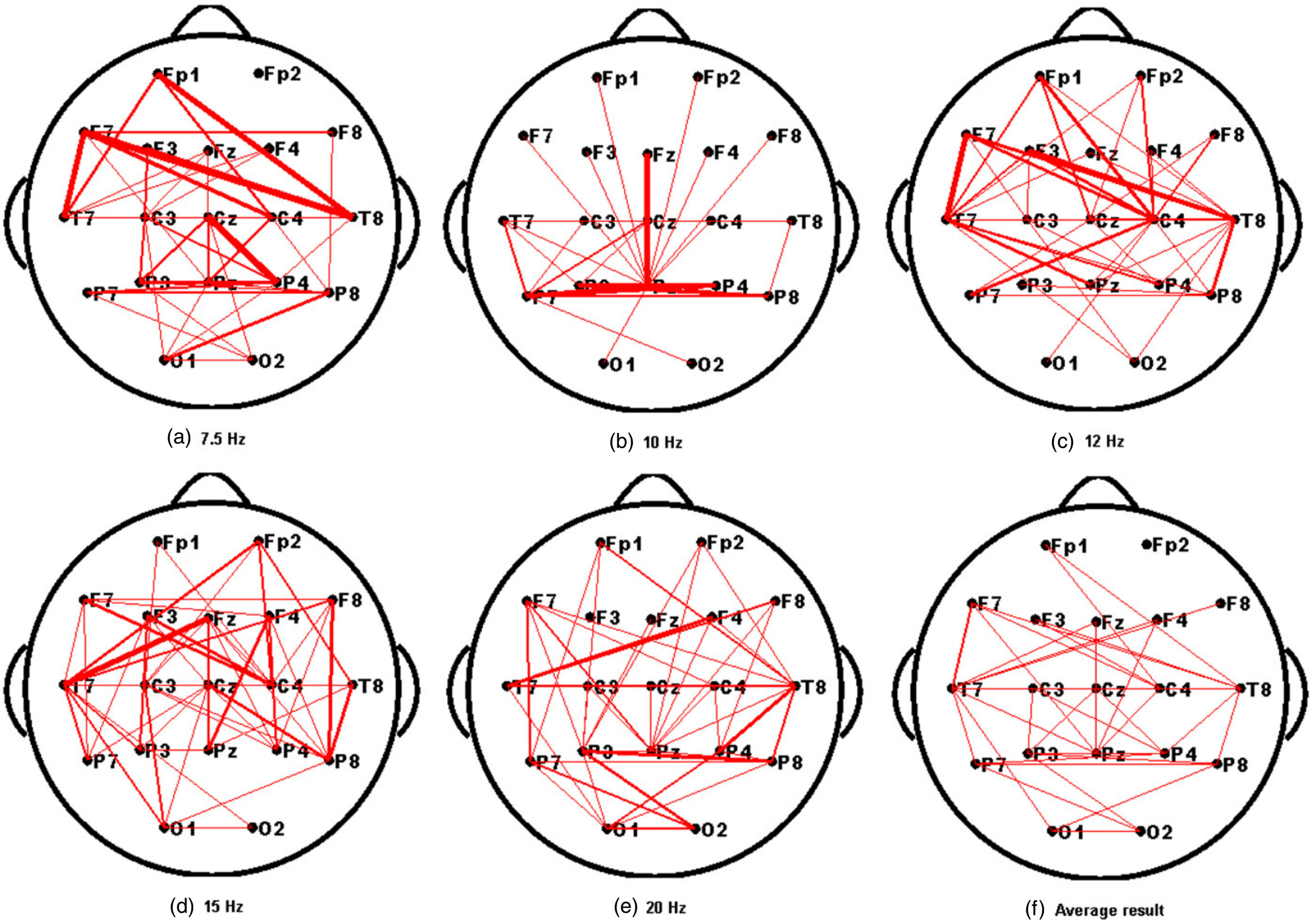

Figure 2. The correlation between the connection strength of each connection and the SNRs across subjects. (a) 7.5 Hz, (b) 10 Hz, (c) 12 Hz, (d) 15 Hz, (e) 20 Hz, (f) average result across the five frequencies. The line width indicates the magnitude of the positive correlation coefficients.

Table 2. The relationships between the topological properties and the SNRs. *r* denotes the correlation coefficient, and *p* denotes the significant level of the correlation coefficient.

	Clustering coefficient		Characteristic path length	
Frequency	r	p	r	p
7.5 Hz	−0.779	0.003	0.741	0.006
10 Hz	−0.542	0.069	0.581	0.047
12 Hz	−0.686	0.014	0.842	0.001
15 Hz	−0.706	0.010	0.746	0.005
20 Hz	−0.699	0.011	0.780	0.003

negatively correlated with the clustering coefficient of the corresponding resting networks, and the SNRs of 10 Hz were marginally significantly correlated with the clustering coefficient of 10 Hz resting networks. For all the five frequencies, the SNRs were significantly positively correlated with the characteristic path length of the corresponding resting networks. Furthermore, we found the averaged clustering coefficient and averaged characteristic path length of the five resting networks respectively showed significantly negative and positive correlations with the average SNRs of the five frequencies across subjects, as shown in figures 4(e), (f).

3.4. The relationship between classification performance and topology measures

Previous studies have demonstrated that high SNRs can improve classification performance [30, 31]. We computed the correlation between the SNRs and classification performance, and got a similar result as shown in figure 5. This result shows that classification accuracy is significantly correlated to the SNRs. The SSVEP data with higher averaged SNR can yield better classification performance. Accordingly, we should choose the stimulus frequencies which can evoke robust SSVEP data (high SNRs) when we design a SSVEP-based BCI system.

For BCI application, the prediction of the performance using the resting-state data is an important topic [16, 17]. It is valuable to investigate whether resting-state network topology can be a candidate performance predictor for SSVEP-based BCI. With the correlation analysis, it is interesting that the three topological measures showed strong correlation with the classification accuracy (table 3). With the regression analysis, the results were comparable to the correlation analysis: the mean functional connectivity (R^2 = 0.348, p = 0.044), the characteristic path length (R^2 = 0.400, p = 0.027) and the clustering coefficient (R^2 = 0.289, p = 0.071) could

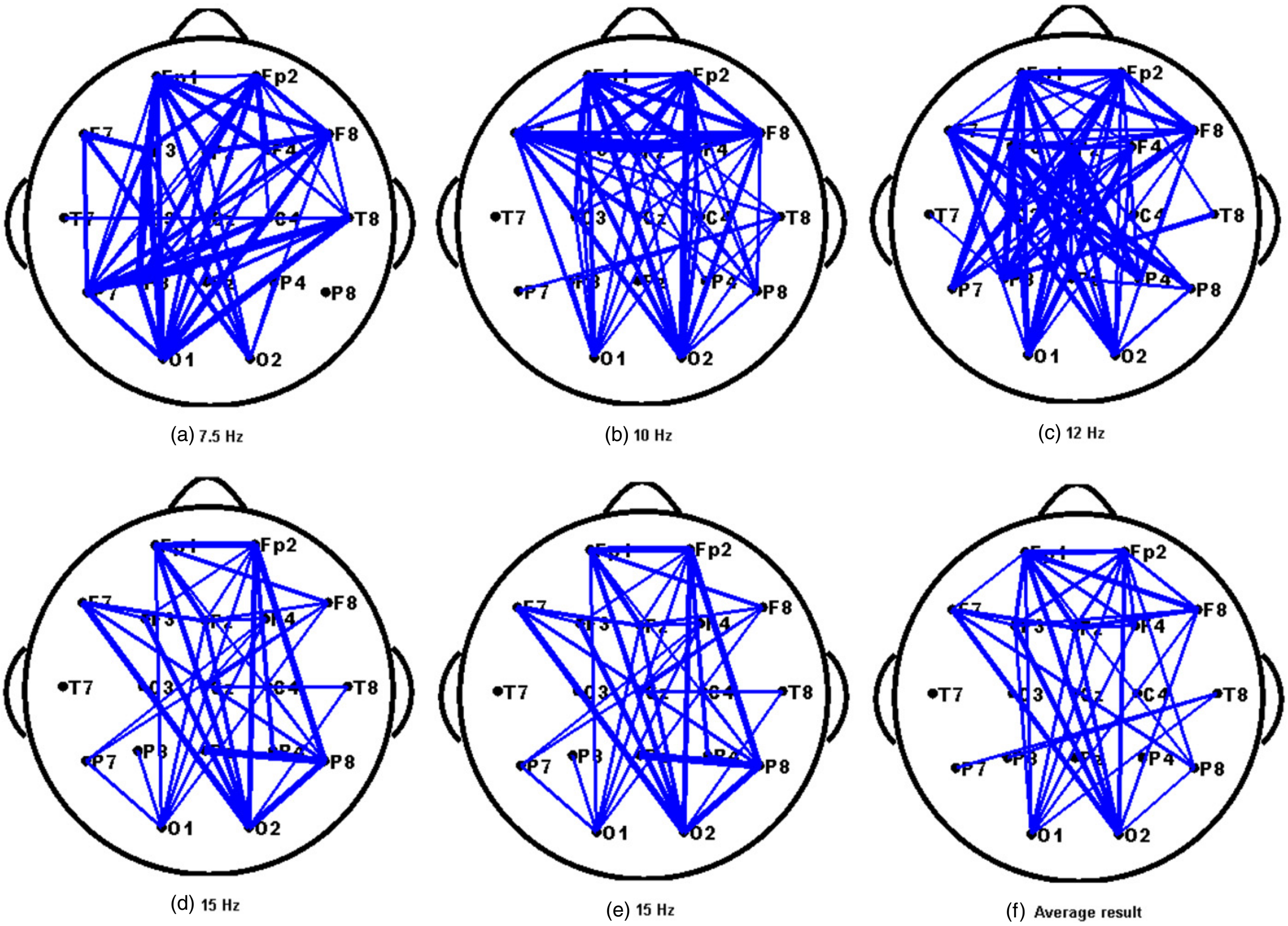

Figure 3. The correlation between the connection strength of each connection and the SNRs across subjects. (a) 7.5 Hz, (b) 10 Hz, (c) 12 Hz, (d) 15 Hz, (e) 20 Hz, (f) average result across the five frequencies. All the absolute values of the correlation coefficients are equal to or larger than 0.4. The line width indicates the magnitude of the absolute values of the negative correlation coefficients.

Table 3. The correlation between the classification accuracy and the averaged topological measures across the four frequencies. r denotes correlation coefficient, and p denotes the significant level of the correlation coefficient.

Measures	r	p
Averaged mean functional connectivity	−0.589	0.043
Averaged clustering coefficient	−0.538	0.071
Averaged characteristic path length	0.633	0.027

serve as feasible predictors. Probably due to the relatively small sample size and the appearance of some outliers, the effectiveness of the performance predictor is limited. Furthermore, we considered whether combinations of the three measures can improve the prediction performance. As the results show in figure 4 and table 3, the mean functional connectivity and clustering coefficient have inverse relations with the accuracies comparing to the characteristic path length. Therefore, we took two routes to solve the problem, i.e. we calculated the reciprocals of mean functional connectivity and clustering coefficient, or the reciprocals of characteristic path length. Before combination, these values were normalized. Each measure of each subject was divided by the summation of the same measures across the subjects. We also used regression analysis to validate our ideas. The results are shown in table 4. It seems that most combinations can provide better prediction performance. Among these combinations, the clustering coefficient and the reciprocals of characteristic path length demonstrate the best performance, which could serve as the predictors more feasibly than other combinations.

Table 4. The prediction performances with different combinations of topological measures. NCC is the normalized clustering coefficient, and INCC is the normalized reciprocals of the clustering coefficient. INPL is the normalized characteristic path length, and INCC is the normalized reciprocals of characteristic path length. NMC is the normalized clustering coefficient, and INMC is the normalized reciprocals of mean coherence. R^2 and p denote the R-square value and the p value with regression analysis.

Combinations	R^2	p
NCC+INPL	0.763	0.002
NMC+INPL	0.758	0.002
NMC+NCC	0.704	0.004
INCC+NPL	0.742	0.002
INMC+NPL	0.743	0.002
NCC+ NMC+INPL	0.763	0.007
INCC+INMC+NPL	0.743	0.009

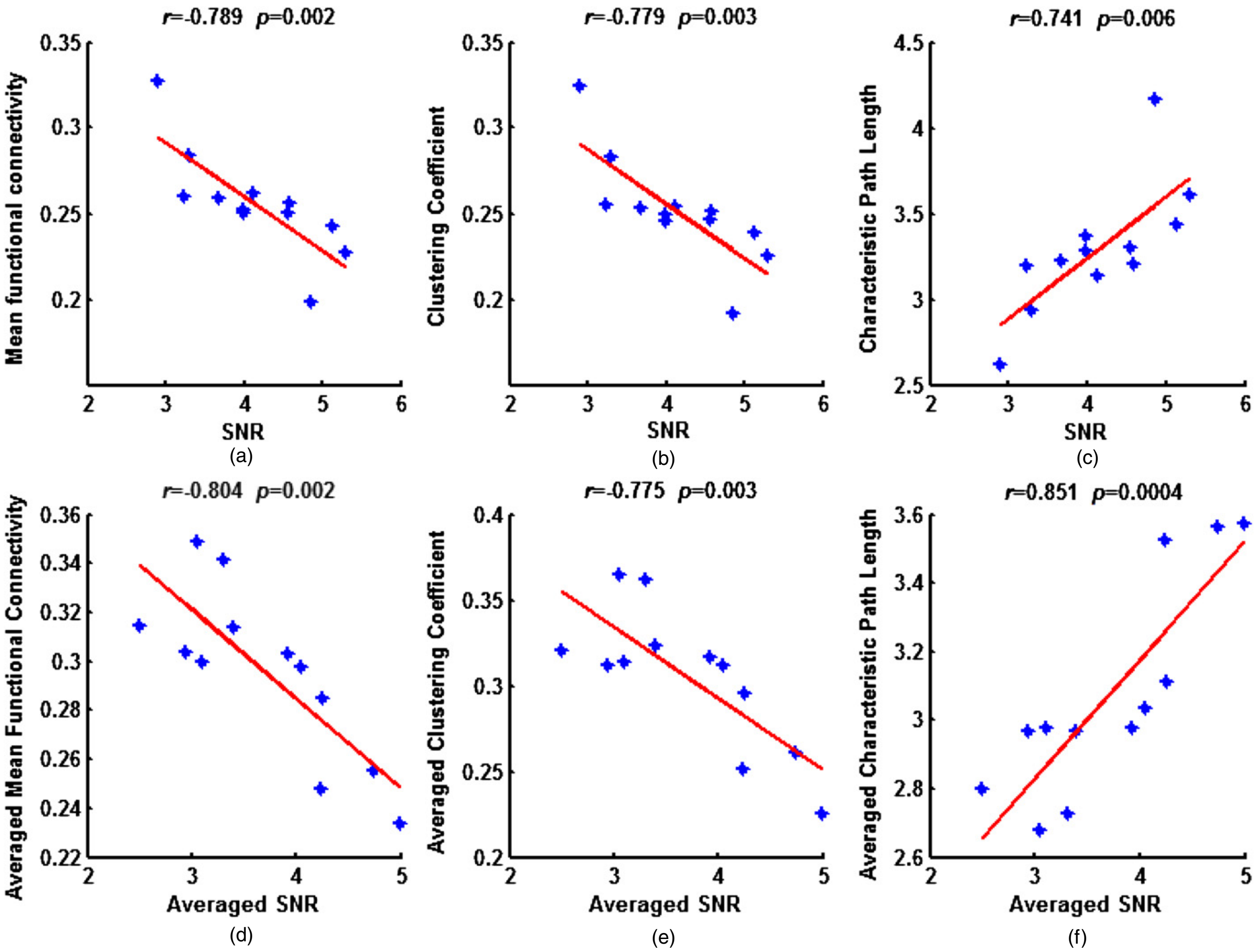

Figure 4. The correlation between the network measures and the SNRs. The first row presents the results of 7.5 Hz; the second row presents the results averaged across the five frequencies. From left to right, these are the relationships between the SNRs and the mean functional connectivity, the clustering coefficient and the characteristic path length respectively. *r* denotes the correlation coefficient and *p* denotes the significant level of the correlation coefficient. The red lines represent the fitted trend lines.

3.5. The results of the PSD-based method

In order to directly compare the proposed method with the PSD-based method, we used a similar approach to [16] to analyze our data. The same frequency bands of interest were used: thetaLow (3.5–6.5 Hz), thetaHigh (6.5–7.5 Hz), alphaLow (7.5–9 Hz), alphaHigh (9–12.5 Hz); betaLow (12.5–18 Hz), betaMid (18–24 Hz), betaHigh (18–30 Hz). The totalSpectrum frequency band in the current study was 1–100 Hz. First, for the nine electrodes (P3, Pz, P4, PO3, POz, PO4, O1, Oz, O2), the relative PSD of each frequency band was calculated in each epoch by FFT. The relative PSD was the PSD of each frequency band divided by the PSD of the totalSpectrum frequency band. Second, we calculated the mean relative PSDs for the Oz across the epochs as in [16], and also calculated the mean relative PSDs across the epochs and the nine electrodes. Third, we calculated the correlation coefficients between the mean relative PSDs of each frequency band and the classification accuracy. The results are shown in table 5. We found that only the mean relative PSDs in the alphaHigh frequency band showed almost significant (for Oz) or significant (for the nine electrodes) correlation with the classification accuracy. The mean relative PSDs averaged across the nine electrodes seem to improve the results. We did not find that the mean relative PSDs in the thetaHigh and betaMid frequency bands were significantly correlated with the classification accuracy as in [16]. It seems that the predictors

Table 5. The correlation between the classification accuracy and the mean relative PSDs of the seven frequency bands. *r* denotes the correlation coefficient, and *p* denotes the significant level of the correlation coefficient.

	Oz		Nine electrodes	
Frequency band	*r*	*p*	*r*	*p*
ThetaLow	0.287	0.365	0.414	0.181
ThetaHigh	−0.057	0.861	−0.067	0.837
AlphaLow	0.014	0.966	0.114	0.725
AlphaHigh	−0.535	0.073	−0.638	0.026
BetaLow	0.454	0.138	0.417	0.177
BetaMid	0.387	0.213	0.398	0.200
BetaHigh	0.461	0.132	0.450	0.142

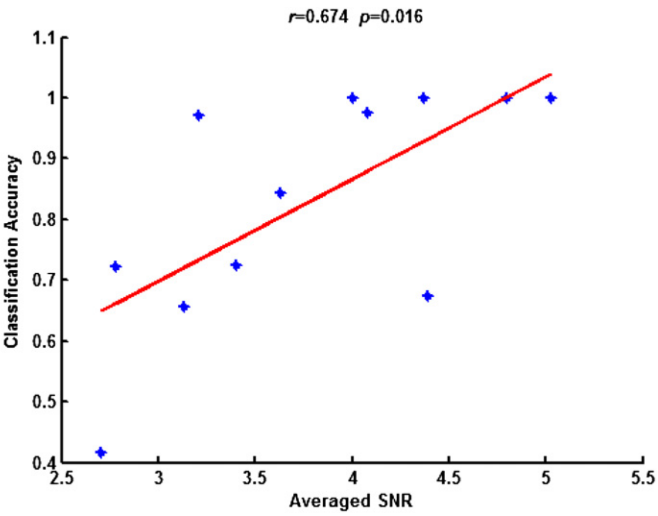

Figure 5. The correlation between the classification accuracy and the averaged SNRs across the four frequencies. *r* denotes the correlation coefficient and *p* denotes the significant level of the correlation coefficient.

may change with the stimulus frequency sets. Therefore, the PSD-based method may not provide predictors which were directly related with the stimulus frequencies. Based on the results shown in tables 3, 4 and 5, the proposed method seems to yield better results than the PSD-based method.

4. Discussion and conclusion

Previous studies have indicated that the resting-state reflects the potential processing abilities of the brain; there are significant associations between cognitive function and resting-state brain network topology [8, 11, 12]. A resting-state fMRI study indicated strong positive associations between the intellectual performance and the global efficiency of brain networks [8]. Owing to the high temporal resolution of EEG and MEG, the researchers explored the association between the cognition and different frequency bands. Zhou *et al* showed that shorter reaction time is correlated with a shorter characteristic path length in gamma band networks using resting-sate EEG [11], and Douw *et al* using resting-state MEG, showed that an increased clustering coefficient in delta, theta and gamma bands was correlated to better cognition [12].

These studies inspire us to adopt the resting-state network measures to evaluate BCI performance. In the present study, we investigated the association between the resting-state network topology and SSVEP responses, and the feasibility of resting-state network topology as the predictor for SSVEP-based BCI. The results confirmed that both resting-state EEG functional network topological properties and mean functional network connectivity were correlated with the SSVEP responses. Interestingly, our results also suggested that these network measures might serve as feasible candidates of performance predictors for the SSVEP-based BCI. Larger SNRs and classification accuracy corresponded to a smaller clustering coefficient and mean functional connectivity, but a larger characteristic path length of the resting-state networks. Furthermore, combinations of the topological measures could provide better prediction results; the clustering coefficient and the reciprocals of characteristic path length demonstrate the best performance.

In this study, the larger SNRs correspond to smaller clustering coefficients, but longer characteristic path lengths of the resting-state networks. It is known that a brain network is less efficient when it has a smaller clustering coefficient and longer characteristic path length [9, 32]. From table 1, we can see that resting-state networks may be task-negative networks. Studies have shown that the stimulus-induced activities are negatively correlated with the activities of the task-negative networks [33]. The negative correlation of SSVEP strength with the resting-state network efficiency may account for a similar physiological basis. A less efficient background network would facilitate SSVEP generation. It has been proved that SSVEP is a resonance response from the functional networks with the same resonance (preferred) frequency as the stimulus [29, 34]. The flickering stimulus plays the role of organizing the rhythms in the brain [34, 35]. Therefore, we may infer that less efficient background processing networks may be easily entrained by the stimulus to show larger synchronization to the flickering stimulus, and then generate relatively greater driving responses to the same stimulus. Accordingly, the topological differences of the resting-state networks may give some explanation for the inter-individual differences of SSVEP responses and BCI performances. Although many factors (for example, attention, fatigue, etc) can lead to the differences of SSVEP responses, we recently found that inter-subject variability is significantly correlated with the topology of the functional networks entrained by periodic stimuli [28]. Both our studies may also support the significance of complex brain network topological parameters [6].

To the best of our knowledge, although the association between resting-state EEG measures and subjects' BCI performances has been investigated [16], this is the first study that explored the association between resting-state EEG activities and SSVEP from a network perspective. For the first time, we found significant associations between the three network measures of resting-state networks and SSVEP, and then we also found that these network measures can play potential roles in performance prediction in SSVEP-BCI. In a recent study, Fernandez-Vargas *et al* found the mean relative PSDs in some of the interesting frequency bands (thetaHigh and betaMid) were related to the BCI performance [16]. First, we think that both the PSD-based method and the network measure-based method provide new evidences of the feasibility of predicting BCI performance with resting-state EEG measures. Both methods could hold potential for improving the SSVEP-based BCI, and can be helpful to better understand the mechanism of generating steady-state evoked brain responses in the brain. Second, these two methods use different measures as the predictors. In the study of Fernandez-Vargas *et al* [16], the frequencies were 20–39 Hz, and the predictors were the mean relative PSDs of thetaHigh and betaMid. However, we do not know whether these predictors can be generalized for other frequencies. In the current study, we found that these predictors could not serve as the predictors for the four frequencies used by us. Only the mean relative PSDs of the alphaHigh showed significant correlation with the classification accuracy. For our proposed method, the network measures are directly related with the stimulus frequencies. Third, according to the results and explanations [16], the PSD-based method may suffer from the size of the sample (small), and different channels may yield different performances. Because users have shown large inter-variation in the SSVEP amplitude and distribution [29], the PSD-based method may need to search the channel which can provide the best prediction performance. Certainly, a PSD-based method may need fewer channels after the channel selection. In table 5, we found that the mean relative PSDs of the alphaHigh averaged across the nine electrodes seemed to improve the results. Therefore, the development of a more robust and efficient method based on PSDs needs further study. For our method, all the used channels work together to generate the network measures, and then the combination of the clustering coefficient and the reciprocals of characteristic path length showed good performance. This phenomenon is similar to the difference between the multichannel frequency recognition method and the single channel frequency recognition method [36]. Fourth, the computation of the network measures was based on the single frequency of the flickering stimulus, not the frequency bands. More studies are needed to further explore the relationship between these two methods; it is also possible to combine both methods to give a more efficient and practical predictor.

The predictability of SSVEP response based on resting-state network measures may be used to screen the subjects [37]. These results may provide new insights to the brain mechanism of BCI, especially for SSVEP-based BCI. Based on our method, we may compute resting-state network measures of a set of frequencies, and then search the optimal frequency combination according to the averaged network measures (i.e. the clustering coefficient and the reciprocals of characteristic path length). In the future, we will verify the feasibility of frequency selection with the other protocols such as the one proposed by Fernandez-Vargas *et al* [16].

In our current study, the results were generated under exactly the same frequencies as the stimulus frequencies, not based on the specific frequency bands (theta, alpha, beta and gamma, etc). First, it could be helpful to better understand the mechanism of generating steady-state evoked brain response in the brain. Second, these measures may be directly related to SSVEP-based BCI parameters, such as stimulus frequencies, which may have more direct application values. It will be also interesting to use specific frequency bands. In future, we will use specific frequency bands to investigate the associations between network properties of resting-state networks and SSVEP, and verify whether some network properties of specific frequency bands can also be used for the performance prediction of SSVEP-based BCI.

It should be noted that we only adopted closed-eye EEG data in this study. Thus, the findings could not be simply generalized to the open-eyed data because some studies have shown differences between the two kinds of resting-state EEG activities [38, 39]. Investigating the relationship between open-eyed resting-state network measures and SSVEP responses and BCI performance would be of great interest to our future study. Volume conduction is another important aspect which should be considered when performing the analysis for the scalp EEG networks. We tried to reduce this influence by choosing nineteen widely-spaced electrodes that cover most of the brain regions. Finally, reference is another important issue that may influence network construction. In this work, we adopted the novel REST method to reduce the reference effect and volume conduction [40–42]. REST using a point at infinity for a reference has the promise of helping reduce or eliminate reference problems, and is a promising method that can avoid the limitations of common references (e.g., inflation of coherence) [41, 42].

In the current study, we only used coherence to construct the resting-state networks. Because SSVEP is a narrow band response ($<$0.1 Hz) centered on the stimulus frequency, coherence may be the best choice to construct the resting-state networks of the stimulus frequency. It will be also important to check whether different measures (e.g. correlation, phase lag index, etc) yield the same results when we construct the resting-state networks. In the future, we will use different measures when we adopt the specific frequency bands to explore the associations between the resting-state network measures and SSVEP, and test the effects and consistencies of the different measures.

In conclusion, the results in this study clearly indicate that both the topological properties and mean function connectivity of the resting-state networks were related to SSVEP responses and performance in SSVEP-based BCI. We believe that our study can shed more light on the studies of SSVEP-based BCI. The proposed method may be helpful to better understand the mechanism of the SSVEP, and also hold potential for improving SSVEP-based BCI.

Acknowledgments

The manuscript was substantially improved thanks to the thoughtful comments of two anonymous reviewers. We sincerely thank Lanjin Guo and Kang Xie for the help in data collection. This work was supported by the 973 project (no. 2011CB707803), the 863 project (no. 2012AA011601) and NSFC (no. 31070881, no. 91232725, no. 61175117 and no. 61201278), and in part by the 111 project and PCSIRT.

References

[1] Regan D 1989 *Human Brain Electrophysiology: Evoked Potentials and Evoked Magnetic Fields in Science and Medicine* (New York: Elsevier)

[2] Vialatte F B, Maurice M, Dauwels J and Cichocki A 2010 Steady-state visually evoked potentials: focus on essential paradigms and future perspectives *Prog. Neurobiol.* **90** 418–38

[3] Nicolas-Alonso L F and Gomez-Gil J 2012 Brain computer interfaces, a review *Sensors* **12** 1211–79

[4] Yin E *et al* 2013 A novel hybrid BCI speller based on the incorporation of SSVEP into the P300 paradigm *J. Neural Eng.* **10** 026012

[5] Xu M *et al* 2013 A hybrid BCI speller paradigm combining P300 potential and the SSVEP blocking feature *J. Neural Eng.* **10** 026001

[6] Zhang Z *et al* 2011 Altered functional–structural coupling of large-scale brain networks in idiopathic generalized epilepsy *Brain* **134** 2912–28

[7] Yao Z *et al* 2010 Abnormal cortical networks in mild cognitive impairment and Alzheimer's disease *PLoS Comput. Biol.* **6** e1001006

[8] van den Heuvel M P, Stam C J, Kahn R S and Hulshoff Pol H E 2009 Efficiency of functional brain networks and intellectual performance *J. Neurosci.* **29** 7619–24

[9] Li Y *et al* 2009 Brain anatomical network and intelligence *PLoS Comput. Biol.* **5** e1000395

[10] Varela F, Lachaux J P, Rodriguez E and Martinerie J 2001 The brainweb: phase synchronization and large-scale integration *Nature Rev. Neurosci.* **2** 229–39

[11] Zhou G *et al* 2012 Interindividual reaction time variability is related to resting-state network topology: an electroencephalogram study *Neuroscience* **202** 276–82

[12] Douw L *et al* 2011 Cognition is related to resting-state small-world network topology: an magnetoencephalographic study *Neuroscience* **175** 169–77

[13] Murias M, Swanson J M and Srinivasan R 2007 Functional connectivity of frontal cortex in healthy and ADHD children reflected in EEG coherence *Cereb. Cortex* **17** 1788–99

[14] Ramos-Loyo J, Gonzalez-Garrido A A, Amicus C and Guevara M A 2004 Relationship between resting alpha activity and the ERPs obtained during a highly demanding selective attention task *Int. J. Psychophysiol.* **54** 251–62

[15] Williams J J, Rouse A G, Thongpang S, Williams J C and Moran D W 2013 Differentiating closed-loop cortical intention from rest: building an asynchronous electrocorticographic BCI *J. Neural Eng.* **10** 046001

[16] Fernandez-Vargas J, Pfaff H U, Rodriguez F B and Varona P 2013 Assisted closed-loop optimization of SSVEP-BCI efficiency *Front Neural Circuits* **7** 27

[17] Blankertz B *et al* 2010 Neurophysiological predictor of SMR-based BCI performance *Neuroimage* **51** 1303–9

[18] Yao D 2001 A method to standardize a reference of scalp EEG recordings to a point at infinity *Physiol. Meas.* **22** 693–711

[19] Srinivasan R, Bibi F A and Nunez P L 2006 Steady-state visual evoked potentials: distributed local sources and wave-like dynamics are sensitive to flicker frequency *Brain Topogr.* **18** 167–87

[20] Lin Z, Zhang C, Wu W and Gao X 2006 Frequency recognition based on canonical correlation analysis for SSVEP-based BCIs *IEEE Trans. Biomed. Eng.* **54** 1172–6

[21] Zhang Y *et al* 2012 Multiple frequencies sequential coding for SSVEP-based brain-computer interface *PLoS One* **7** e29519

[22] Wang Y T, Wang Y and Jung T P 2011 A cell-phone-based brain-computer interface for communication in daily life *J. Neural Eng.* **8** 025018

[23] Bin G, Gao X, Yan Z, Hong B and Gao S 2009 An online multi-channel SSVEP-based brain-computer interface using a canonical correlation analysis method *J. Neural Eng.* **6** 046002

[24] Rubinov M and Sporns O 2010 Complex network measures of brain connectivity: uses and interpretations *Neuroimage* **52** 1059–69

[25] Onnela J P, Saramaki J, Kertesz J and Kaski K 2005 Intensity and coherence of motifs in weighted complex networks *Phys. Rev.* E **71** 065103

[26] Watts D J and Strogatz S H 1998 Collective dynamics of 'small-world' networks *Nature* **393** 440–2

[27] Newman M E J 2003 The structure and function of complex networks *SIAM Rev.* **45** 167–256

[28] Zhang Y, Xu P, Huang Y, Cheng K and Yao D 2013 SSVEP response is related to functional brain network topology entrained by the flickering stimulus *PLoS One* **8** e72654

[29] Srinivasan R, Fornari E, Knyazeva M G, Meuli R and Maeder P 2007 fMRI responses in medial frontal cortex that depend on the temporal frequency of visual input *Exp. Brain Res.* **180** 677–91

[30] Wang Y, Wang R, Gao X, Hong B and Gao S 2006 A practical VEP-based brain-computer interface *IEEE Trans. Neural Syst. Rehabil. Eng.* **14** 234–9

[31] Zhu D, Bieger J, Garcia Molina G and Aarts R M 2010 A survey of stimulation methods used in SSVEP-based BCIs *Comput. Intell. Neurosci.* **2010** 702357

[32] Stam C J and Reijneveld J C 2007 Graph theoretical analysis of complex networks in the brain *Nonlinear Biomed. Phys.* **1** 3

[33] Northoff G, Qin P and Nakao T 2010 Rest-stimulus interaction in the brain: a review *Trends Neurosci.* **33** 277–84

[34] Lazarev V V, Simpson D M, Schubsky B M and Deazevedo L C 2001 Photic driving in the electroencephalogram of children and adolescents: harmonic structure and relation to the resting state *Braz. J. Med. Biol. Res.* **34** 1573–84

[35] Gevins A 1993 High resolution EEG *Brain Topogr.* **5** 321–5

[36] Friman O, Volosyak I and Graser A 2007 Multiple channel detection of steady-state visual evoked potentials for brain-computer interfaces *IEEE Trans. Biomed. Eng.* **54** 742–50

[37] Allison B *et al* 2010 BCI demographics: how many (and what kinds of) people can use an SSVEP BCI? *IEEE Trans. Neural Syst. Rehabil. Eng.* **18** 107–16

[38] Chen A C, Feng W, Zhao H, Yin Y and Wang P 2008 EEG default mode network in the human brain: spectral regional field powers *Neuroimage* **41** 561–74

[39] Barry R J, Clarke A R, Johnstone S J, Magee C A and Rushby J A 2007 EEG differences between eyes-closed and eyes-open resting conditions *Clin. Neurophysiol.* **118** 2765–73

[40] Marzetti L, Nolte G, Perrucci M G, Romani G L and Del Gratta C 2007 The use of standardized infinity reference in EEG coherency studies *Neuroimage* **36** 48–63

[41] Thatcher R W 2012 Coherence, phase differences, phase shift, and phase lock in EEG/ERP analyses *Dev. Neuropsychol.* **37** 476–96

[42] Qin Y, Xu P and Yao D 2010 A comparative study of different references for EEG default mode network: the use of the infinity reference *Clin. Neurophysiol.* **121** 1981–91